

Research Article

Evaluation of the Can Gio Vegetation Index changes using the Sentinel-2 Datasets from 2015 to 2023

Anh Bui Khanh Van^{1*}

¹ Ho Chi Minh City University University of Natural Resources and Environment;
bkvanh@hcmunre.edu.vn; bkvanh2020@gmail.com

*Corresponding author: bkvanh2020@gmail.com; Tel.: +84–908836115

Received: 27 October 2023; Accepted: 4 December 2023; Published: 25 March 2024

Abstract: Can Gio Mangrove Biosphere Reserve provide many ecosystem services, such as provisioning, regulating, cultural, and supporting services for the urban areas as well as wildlife of suburban areas in Ho Chi Minh City and the nearby ecosystems. Therefore, it is important to monitor and evaluate the change of mangrove forest cover in the long term. In this study, the Normalized Difference Vegetation Index - NDVI at 10 m resolution from 2015 to 2023 of Can Gio was obtained from the Copernicus Sentinel-2 database using Google Earth Engine - GEE. Subsequently, NDVIs statistic were computed by R to assess the slope of NDVI change with p-value significance in Can Gio. The results indicated that NDVI values typically range from -0.4 to +0.8 and vary annually. It is evident that NDVIs values from 2015 to 2020 are marginally higher than those recorded between 2021 and 2023. The degradation in average NDVI from 2015 to 2023 was rationally deducible either from the downsizing of mangrove forest areas or the degradation of the mangrove forest. However, the annual NDVI statistic revealed there were areas with an acceleration of NDVI in comparison with the destruction of NDVI areas from 2015 to 2023. Linear regression effectively models continuous processes like deposition or erosion. However, to evaluate other factors such as discrete human-made or sporadic impacts, alternative statistical models should be considered.

Keywords: Normalized Difference Vegetation Index - NDVI; The Copernicus Sentinel-2 database; Can Gio; Spatial and temporal pattern.

1. Introduction

Can Gio is an important ecosystem in Ho Chi Minh City, not only for historical meaning but also the future development. In the past, a large area of Can Gio was destroyed by herbicides using from 1965 to 1969 and by anthropogenic of local people from 1970 to 1980 [1]. From 1990 to 2000, many projects to reforestation were conducted. After being declared as the first Mangrove Biosphere Reserve (MBR) in Viet Nam in 2000, the studies of Can Gio has been increased and Can Gio has become an important research site [2].

Can Gio Mangrove Biosphere Reserve has provided many ecosystem services, such as provisioning, regulating, cultural, and supporting services for the urban areas as well as wildlife of suburban areas in Ho Chi Minh City and the nearby ecosystem[1]. The mangrove ecosystem in Can Gio serves as a crucial habitat for a diverse range of flora and fauna. Also, mangrove forest act as a natural barrier, protecting the coastline from erosion and minimizing the impact of storm surges. Besides, mangrove trees are highly effective at sequestering carbon dioxide from the atmosphere [2]. The root systems of mangrove filter pollutants and sediment from the water, improving water quality. Among other functions, the role of Can Gio requires a quantitative and complementary assessment.

Can Gio is currently confronted with a combination of human-induced and natural impacts [1,3]. Consequently, monitoring the ongoing changes in Can Gio is crucial for both present management and future development. Previous studies have delineated three primary processes characterizing the water-soil-plant dynamics in Can Gio, including (1) bank erosion stemming from both river systems and seawater; (2) seasonal fluctuations within the mangrove forests; and (3) anthropogenic influences encompassing preservation efforts or induced alterations [4–6].

For instance, Ly Nhon, the largest commune in Can Gio, experiences significant effects from the dynamics of the Dong Tranh River, notably in its near-shore areas. Studies indicate that the riverbank along Dong Tranh experiences considerable deposition, whereas areas draining into the East Sea endure severe erosion processes [4]. Situated between Cape of Dong Tranh and the East Sea borders, Long Hoa faces substantial impacts from waves, coastal storms, and typhoons, causing severe erosion along the commune's borders. Similarly, significant erosion points are observed in Can Thanh, yet constructed infrastructures such as concrete groins and rock dikes have mitigated shoreline erosion. In contrast, Thanh An experiences minimal erosion within Can Gio, although some bank river erosion has been reported [4].

Various studies utilized vegetation indices, such as the Normalized Difference Vegetation Index (NDVI), to gauge the quality of vegetation [2, 7–10]. Nevertheless, the emphasis in most of these studies has been on delineating spatial distribution rather than exploring ongoing temporal fluctuations over a yearly timescale. As such, there is a need to shift focus towards examining the temporal dynamics of vegetation to better understand the evolving conditions in mangrove forests, specifically in Can Gio over time.

Therefore, this study objective is to assess Can Gio vegetation index’s variation across a continuous time series spanning from 2015 to 2023. This analysis infers significance as it employs statistical linear regression method to highlight areas demonstrating noteworthy annual fluctuations, illustrating either substantial increase or decrease in NDVI values at yearly timescale.

2. Materials and Methods

2.1. Study area

Located in the southeastern region of Ho Chi Minh City, Can Gio spans an estimated area of approximately 70,000 hectares, predominantly comprising an expansive mangrove

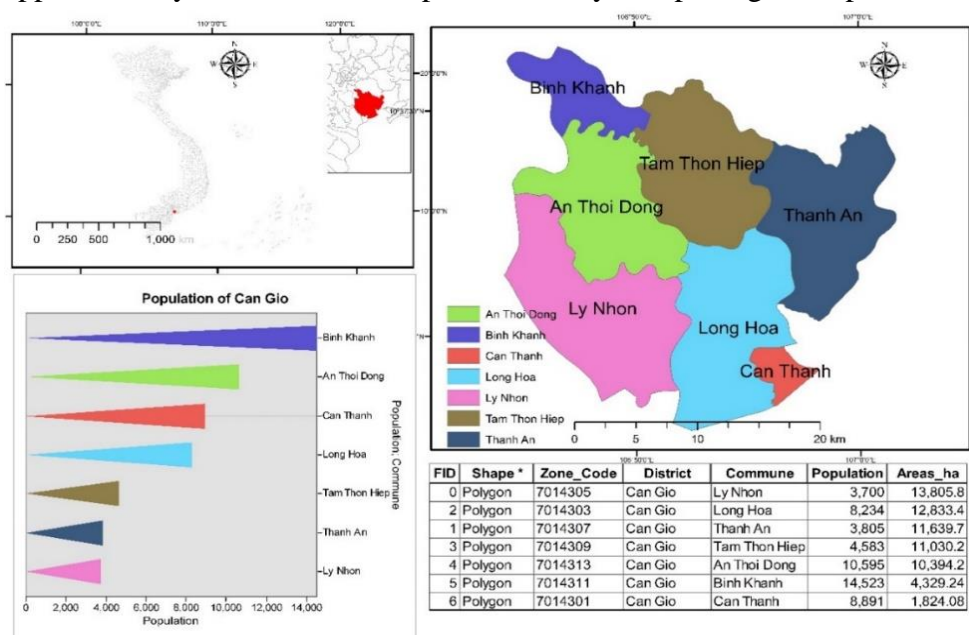


Figure 1. Study area of Can Gio.

forest that is integral to Ho Chi Minh City. This district is intersected by four major rivers Soai Rap, Dong Tranh, Nga Bay (Long Tau), and Thi Vai which course through the Can Gio mangroves before reaching the East Sea. The water bodies cover roughly 22,000 hectares of Can Gio, amounting to approximately 20 percent of its total area [6].

Can Gio encompasses one township, Can Thanh, and is further divided into six communes: Binh Khanh, An Thoi Dong, Ly Nhon, Tam Thon Hiep, Long Hoa, and Thanh An. Notably, Binh Khanh and An Thoi Dong are the two most populous communes, each with populations exceeding 10,000 inhabitants. Can Thanh and Long Hoa have populations exceeding 8,000, while Ly Nhon, Thanh An, and Tam Thon Hiep have the lowest populations, ranging from 3,700 to 4,500 residents (Figure 1).

2.2. Methods

The Copernicus program is a large Earth Observation by the European Union, and it encompasses various satellites, instruments, data services, and applications. The number of satellites in the program may change over time as new satellites are launched and integrated into the system. Some satellites of this program are Sentinel-1A and Sentinel-1B, Sentinel-2A and Sentinel-2B, Sentinel-3A and Sentinel-3B, and many others. In this study, Sentinel-2A and Sentinel-2B were applied to calculate NDVI. Sentinel-2 satellites includes two identical satellites which were respectively launched in 2015 and 2017 at a mean altitude of 786 km. These two satellites operate and provide high-resolution optical imagery for Earth observation and environmental monitoring, including the monitoring of vegetation, soil and water cover, as well as observation of inland waterways and coastal areas [8]. Sentinel-2 offers extensive coverage of vegetation across coastal areas, boasting a superior spatial resolution of 10 meters and frequent revisits every five days. Notably, this satellite service is cost-free, making it a valuable data resource for studying the spatial and temporal dynamics of mangrove forests. Its benefits are particularly significant in developing nations with constrained budgets for such research endeavors [11].

Google Earth Engine is a cloud-based platform designed for global-scale data analysis. It combines a variety of satellite imagery and other geospatial datasets with analysis capabilities by Google's computational infrastructure. In Google Earth Engine, there are multiple datasets of Sentinel-2 such as Sentinel-2 MSI, harmonized Sentinel – 2 MSI. In this study, Sentinel-2 Multi-Spectral Instrument, Level-1C was employed. Each Sentinel-2 product in .zip archive may contain multiple granules. Each granule becomes a separate Earth Engine asset. Earth Engine asset IDs for Sentinel-2 have the following format: COPERNICUS/S2/20230211T030849_20230211T031915_T48PYS. Here the first numeric part represents the sensing date and time which was February 11th, 2023, the second numeric part represents the product generation date and time which was from 03:08:49 to 03:19:15 of the same day, and the final 6-character string is a unique granule identifier indicating its UTM grid reference of Can Gio at T48PYS.

In this study, clouds degree was removed by using Earth Engine code which is “.filterMetadata (“CLOUDY_PIXEL_PERCENTAGE”, “less_than”, 10)”. FilterMetadata is a method used in GEE to filter a collection based on metadata properties. The term “CLOUDY_PIXEL_PERCENTAGE” is the metadata property being used for filtering. It refers to the percentage of cloudy pixels in satellite imagery. The term “less_than” is a comparison operator specifying the filtering condition and 10 is the threshold value of the cloudy pixel percentage.

NDVI stands for Normalized Difference Vegetation Index, it is a fraction of the differences between the reflectance in the near-infrared -NIR and the reflectance in the visible red - RED of the electromagnetic spectrum. NDVI is calculated as in the following formula (1):

$$NDVI = \frac{(NIR-RED)}{(NIR+RED)} \quad (1)$$

NDVI ranges from -1 to +1, in which NDVI values near -1 typically represent water bodies. NDVI values are near 0 representing barren areas, rocks, or built-up urban areas. NDVI values between 0 to 1 indicate varying levels of vegetation density, with higher values suggesting healthier and more dense vegetation [7,12]. NDVIs of Can Gio from 2015 to 2023 were calculated directly on GEE from Sentinel-2 MSI.

The accuracy of NDVI representing land-use types is normally evaluated by Cohen’s Kappa which is a statistical measure that assessed the level of agreement between the interpreted raster and observed raster. In this study, the interpreted raster is the NDVI in 2021 and observed raster is the updated observation in Google Earth.

To calculate the observed agreement and the expected agreement, a confusion matrix was produced with columns and rows. Each row and column respectively represent the classification for raster interpretation. The rows are the classification algorithm, while the columns represent the validation [13, 14].

Then, Kappa efficiency is computed in the formula (2):

$$\kappa = \frac{P_o - P_e}{1 - P_e} \tag{2}$$

where P_o is the observed agreement between rasters, P_e is the expected agreement, which represents the probability of agreement occurring by chance. κ values of 1 indicates perfect agreement; the closer κ values are to 1, the higher consistency between the data [15].

The research method is summarized in the following flow diagram:

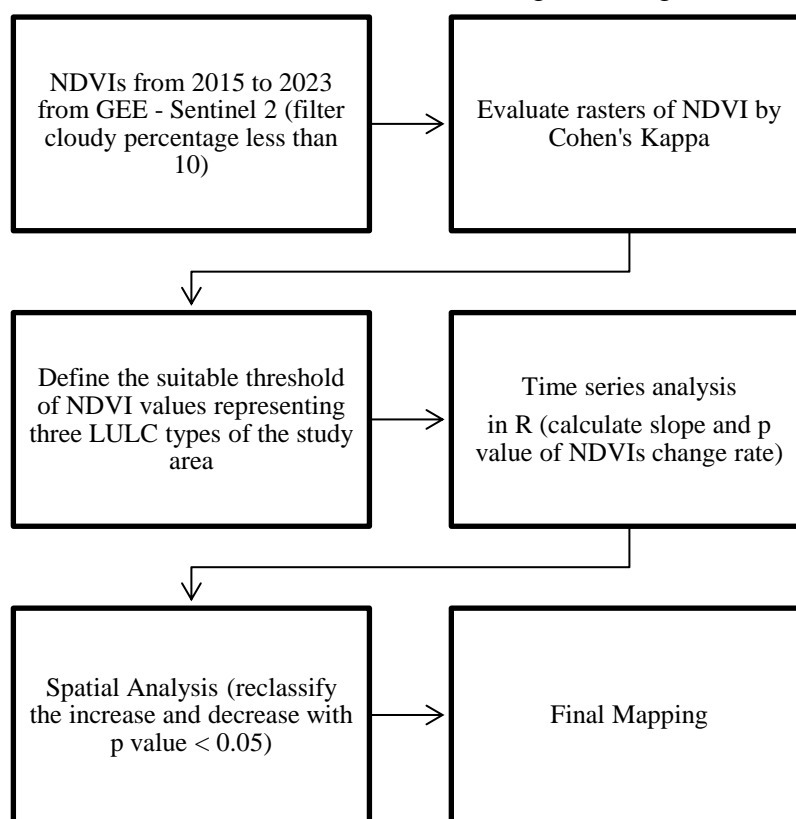


Figure 2. Flow diagram of methodology.

NDVI data spanning from 2015 to 2023 were gathered using GEE's cloud storage tool, specifically filtering the Sentinel-2 dataset to include only data with a cloud cover rate below 10%. This selection predominantly represents NDVI values observed during the dry season. Subsequently, the project adopted an NDVI value index exceeding 0.377 to delineate mangrove forests. It is crucial to assess the accuracy of this interpretation utilizing the Kappa coefficient.

In conducting statistical analysis on the temporal changes in NDVI values for every pixel annually, each pixel comprises 9 NDVI values across consecutive years from 2015 to 2023. The

'raster' package in the R statistical analysis software was employed to compute the slope values representing the upward or downward trends of NDVI for each pixel over the 9-year period, spanning from 2015 to 2023. Due to the extensive dataset, the computation process is time-consuming, given the approximately 7,000,000 pixels for each raster file in each year. Following the computation, a raster map delineating the slope values derived from the analysis model is generated. In addition, the statistical significance assessment - p - value of each slope value for every pixel is also extracted from the statistical model results.

Upon integrating both slope values and the associated p-values for each pixel, the generated map highlights pixels exhibiting significant trends in NDVI. Consequently, the final map delineates areas where NDVI values have consistently risen over 9 consecutive years and those where a consistent decline is simulated. This representation of the raising or reducing trends in NDVI holds paramount importance in identifying specific areas demonstrating sustained growth or decline in NDVI through time.

3. Results and discussion

3.1. NDVIs from 2015 to 2023

NDVIs for Can Gio were calculated as the difference between Band 8 and Band 4, representing the reflectance of near-infrared and visible red light in the electromagnetic spectrum, respectively. NDVI values typically range from -0.4 to +0.8 and vary annually, as in Figure 3a.

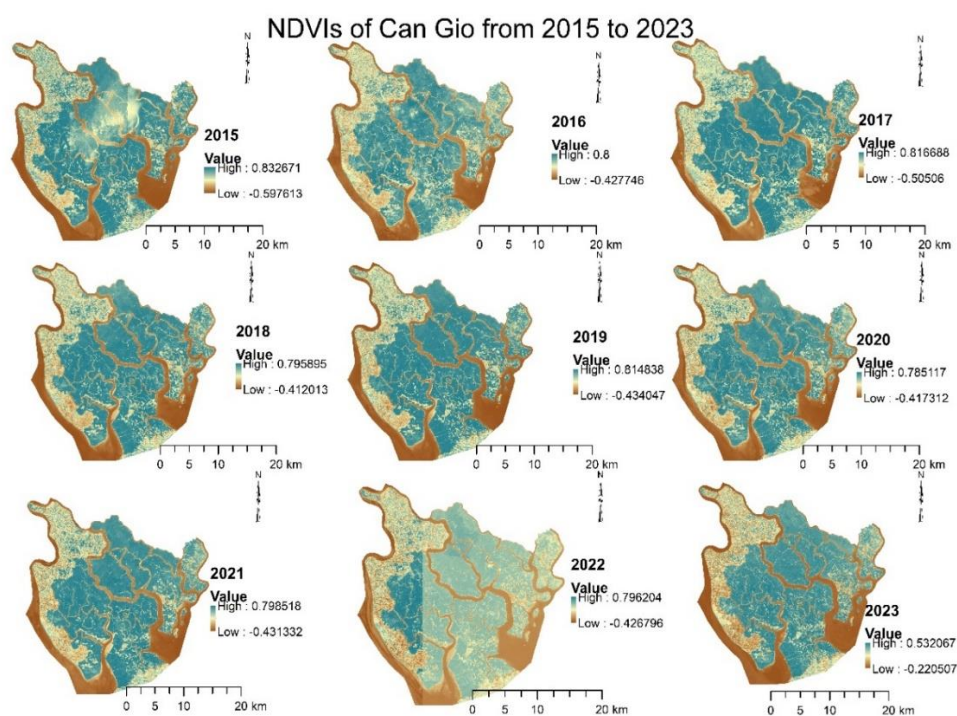


Figure 3a. Annual NDVIs for Can Gio from 2015 to 2023.

The maximum NDVI values for 2015, 2016, 2017, and 2019 exceeded 0.8, whereas those for 2018, 2020, 2021, and 2023 were below 0.8. Specifically, the maximum NDVI in 2023 was recorded at 0.53. These variations highlight the significant impact of annual maximum NDVI values on the overall NDVI average. Regarding the minimum NDVI values, 2015 and 2017, both fell below -0.5, while for 2016, 2018, 2019, 2020, 2021, and 2022, the values were above -0.4. Notably, in 2023, the minimum NDVI reached its highest value of -0.22.

The line graph in Figure 3b illustrates the average yearly NDVI values spanning from 2015 to 2023. It is evident that NDVIs values from 2015 to 2020 are marginally higher than those recorded between 2021 and 2023.

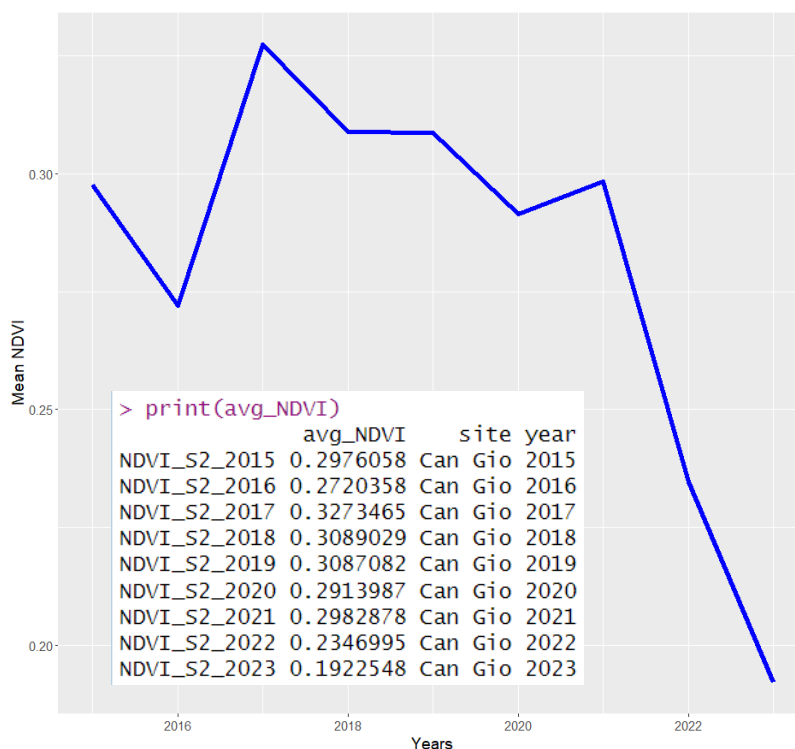


Figure 3b. Average NDVIs for Can Gio from 2015 to 2023.

Typically, NDVIs fluctuated between 0.298 and 0.291 over the 6-year period, while the values of NDVIs considerably diminished from 0.298 in 2021 to 0.192 in 2023. Specifically, the NDVI for 2023 falls within the lowest range. This could be attributed to the fact that the NDVIs for 2023 were collected during the dry season, while the NDVIs for other years reflected values for the entire of year. Similarly, the annual average NDVIs for Can Gio from 2015 to 2023 illustrated a reduction over this period.

3.2. Defining the suitable threshold of NDVI values representing three LULC types

NDVI, widely utilized in studies assessing plant growth, plays a crucial role in vegetation cover classification through various value thresholds. Recently, there have been many studies applying satellite data to identify the vegetation cover. These study have proposed various methods to determine NDVI threshold values to interpret the land-use types for Can Gio. In the estimation conducted by Sugara et al., distinct NDVI thresholds were established for mangroves across three ranges: 0.11 to 0.35 indicating very low vegetation coverage, 0.35 to 0.5 representing medium coverage, and 0.5 to 0.67 signifying high levels of coverage [7].

Among other studies, the NDVI values in the Can Gio mangrove forest area have been classified on a scale ranging from -1 to +0.1999, where values below zero to +0.1999 indicate non-vegetative cover, from +0.2 to +0.2999 signify low vegetation coverage, from +0.3 to +0.3999 represent moderate coverage, and values above +0.4 denote high coverage [11], [16]. Additionally, the author concludes in this study that NDVI values exceeding 0.3 indicate error categorizing areas, partly within the buffer zone [11]. In a separate study, a composite of NDVI and other metrics was employed to assess alterations in mangrove forests. The study categorized NDVI values accordingly: values below 0 indicated bare land, while those between 0 and 0.2 represented low land cover. Ranges of 0.2 to 0.3 indicated shrub and grassland, and higher values, specifically between 0.4 and 0.9, signified dense vegetation coverage [17].

A recent study utilized GEE data from Landsat satellite images to combine the NDVI index with other vegetation assessment indices every five years between 1990 and 2022, aiming to determine vegetation cover. In this study, NDVI threshold adopted the results which were defined in [9] and indicated that majority of vegetation pixels had an NDVI greater than 0.377.

Additionally, other studies indicated that water areas typically exhibit an NDVI less than 0 [4, 9].

To sum up, previous studies focusing on mangrove vegetation and the NDVI index have frequently proposed thresholds around 0.4 to delineate high mangrove forest coverage. Hence, in this particular study, the classification of NDVI values aligns with those determined in prior research, serving as a basis for assessment. Therefore, NDVI values were categorized into three groups: the first group represents water areas with NDVIs less than 0; the second group corresponds to built areas with NDVIs ranging from 0 to 0.377; the third group encompasses mangrove forest areas with NDVIs greater than 0.377.

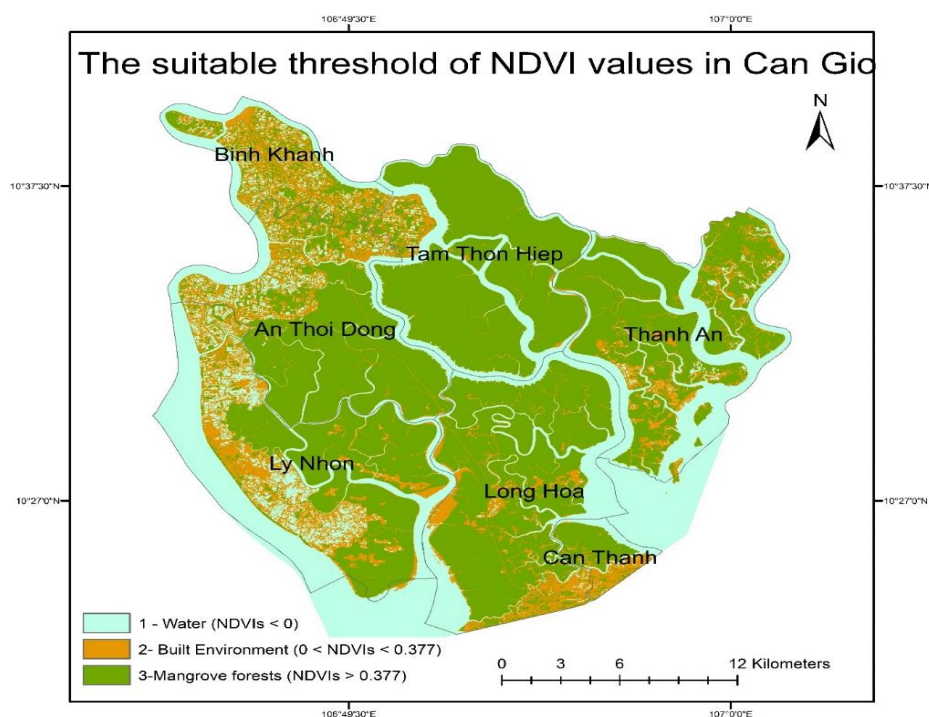


Figure 4. The suitable threshold of NDVI values in Can Gio.

Accordingly, regions with extensive mangrove forest cover predominantly span across Tam Thon Hiep, Thanh An, Long Hoa, and An Thoi Dong communes. Conversely, areas like Binh Khanh, Ly Nhon, and Can Thanh primarily consist of man-made environment. The distributed water surface area corresponds to the primary waterways in the Can Gio area, including Soai Rap, Dong Tranh, Nga Bay (Long Tau), and Thi Vai.

Certain studies utilizing the NDVI index to assess vegetation dynamics in Can Gio have selected random points for accuracy assessment between the simulated land cover results with observed land cover. These studies have proposed varying observation points, ranging from less than 100 points [18] to 300 points [11, 19] or 500 points [9] and over 1,000 [20] sampling points. Some research has computed the number of random points based on a statistically more reliable equation [9].

To evaluate the accuracy for the classification algorithm, 300 random points as in Figure 4 were generated using the segmentation and classification tool in GIS. Subsequently, the point shapefile was converted to a .KML file for potential viewing on Google Earth. Following this, the table of point shapefile was manually edited and compared to the Google Earth Imagery from 2021.

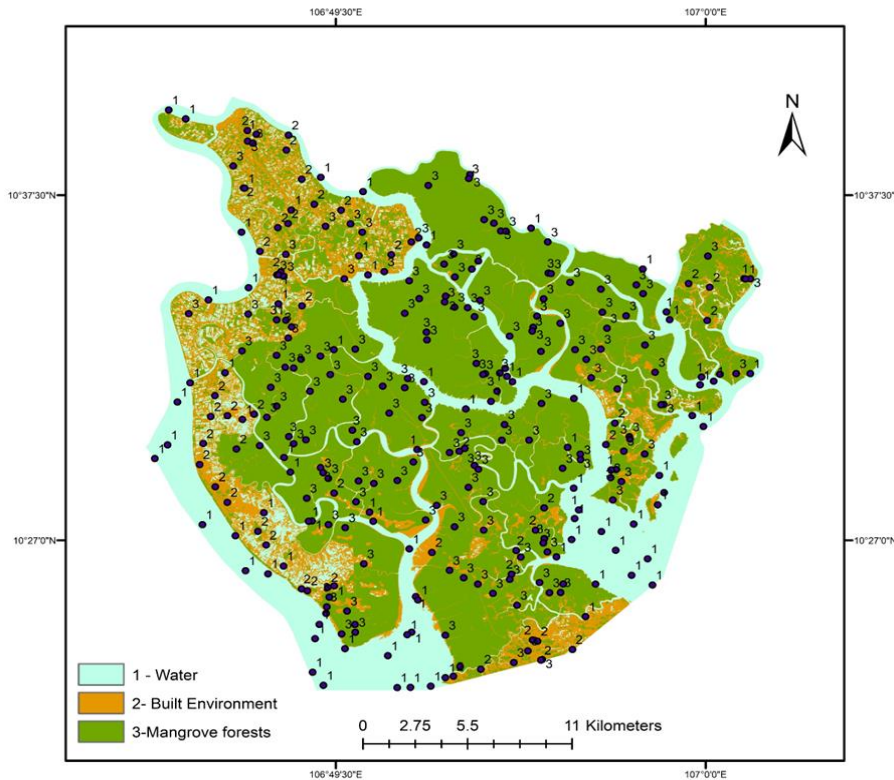


Figure 5. 300 random points for accuracy assessment.

Table 1 shows the confusion matrix result, comparing the results of NDVI classification to Google Earth imagery in 2021 for assessing the accuracy of the proposed classification. The User’s Accuracy (U_Accuracy) reveals that 85% of water, 83% of built areas, and 88% of mangrove forest were correctly classified. Notably, the Producer’s Accuracy (P_Accuracy) for built areas was 57%, significantly lower than that for water areas and mangrove forests, indicating a lower level of correctness in classifying pixels for the built areas. Despite this, the Kappa coefficient was 0.78, suggesting substantial agreement beyond chance.

Table 1. Confusion matrix for NDVI in 2021.

OID	ClassValue	3 –			Total	U_Accuracy	Kappa
		1 –	2 – Built	Mangrove			
		Water	Areas	Forests			
0	1 – Water	76.00	13.00	0.00	89.00	0.85	0.00
1	2 – Built Environment	3.00	39.00	5.00	47.00	0.83	0.00
2	3 – Mangrove Forests	2.00	17.00	145.00	164.00	0.88	0.00
3	Total	81.00	69.00	150.00	<u>300</u>	0.00	0.00
4	P_Accuracy	0.94	0.57	0.97	0.00	0.87	0.00
5	Kappa	0.00	0.00	0.00	0.00	0.00	<u>0.78</u>

3.3. Slope and p-value of NDVIs changing rate from 2015 to 2023

NDVIs from 2015 to 2023 were analyzed through a time series to monitor changes in vegetation over time. Raster data spanning from 2015 to 2023 were stacked into a time series dataset. The slope of the linear regression of NDVI against yearly time was calculated for each pixel, providing valuable insights into the temporal trends. Distribution of slope values and p-values is illustrated in Figure 6. The frequency distribution of slope values less than 0 dominants over that of slope values greater than 0. Distribution of p-values is also depicted, ranging from 0 to 1, where p-values below 0.05 indicate the statistically significant meaning.

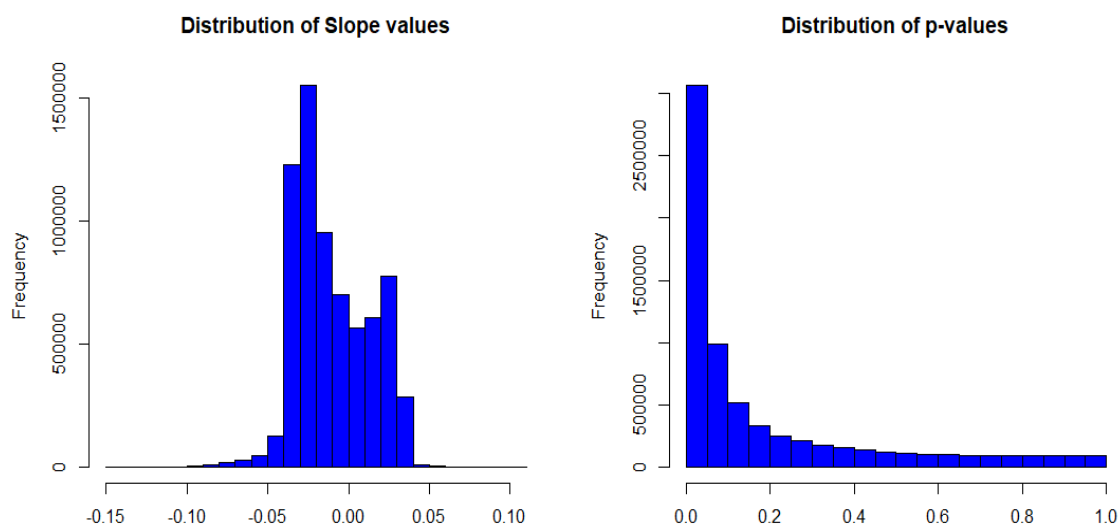


Figure 6. Distribution of slope values and p-values.

However, the p-values of the linear regression for each pixel (Figure 7) were not statistically significant ($p > 0.05$) across a large area, including Binh Khanh, Tam Thon Hiep, An Thoi Dong, and Ly Nhon. In these regions, the observed changed in NDVI over time were not found to be statistically different from zero.

Conversely, statistically significant p - values ($p < 0.05$) were observed at the upper portion of Tam Thon Hiep, Thanh An, Long Hoa, and in most water areas. In these locations, the linear regression analysis provided evidence of a significant trend in NDVI over the study period.

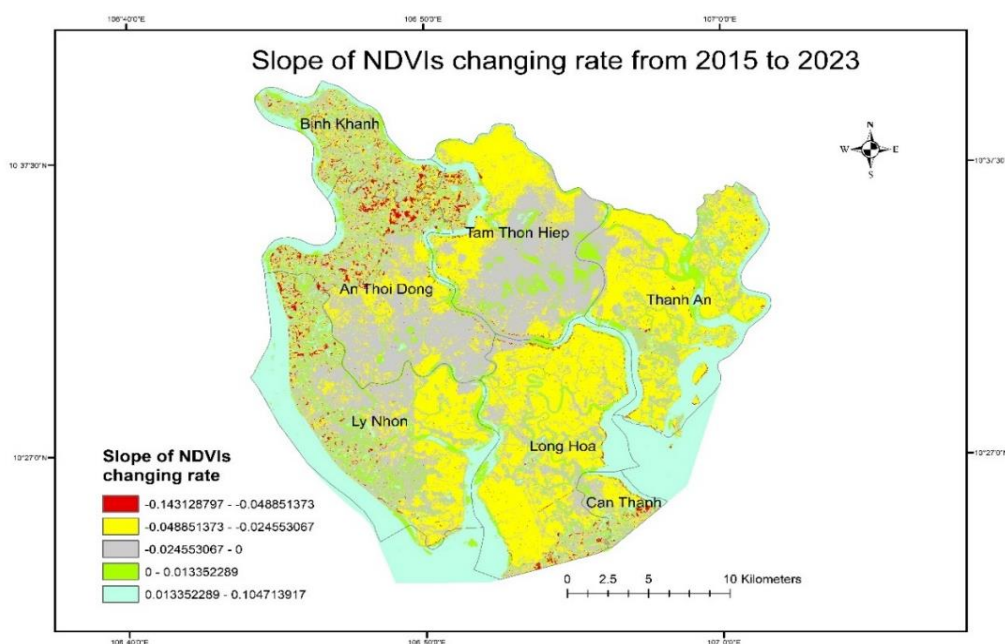


Figure 7a. Slope values of NDVIs changing rate from 2015 to 2023.

The slope raster in Figure 7 was classified into five groups based on specific criteria. Negative slope values indicate a decrease in NDVI, while positive slope values represent an increase. As a result, highly decreases were observed in Binh Khanh, An Thoi Dong, and Can Thanh. Moderately decreases were notable in the buffer zones such as Long Hoa, Thanh An, and the upper of Tam Thon Hiep. On the other hand, the strongly increases were predominately observed in most of water areas and some in Ly Nhon and Tam Thon Hiep.

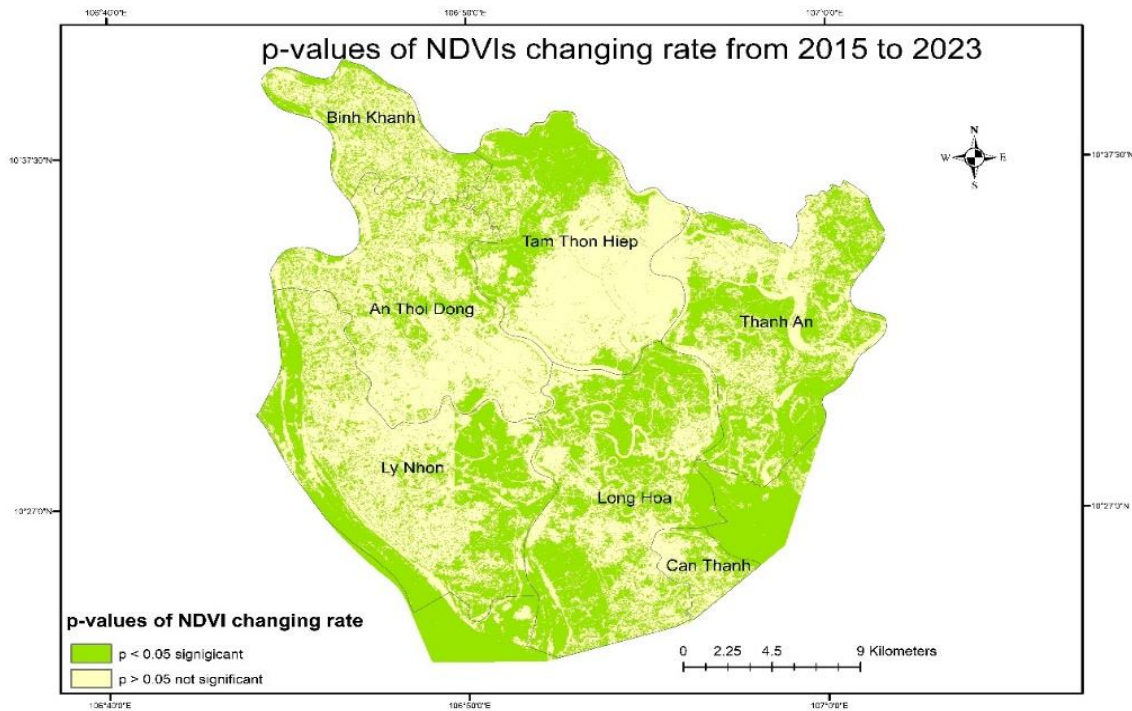


Figure 7b. p-values of NDVIs changing rate from 2015 to 2023.

As a consequence, the map of tendency of NDVI change from 2015 to 2023 was produced to visualize the areas statistically reduction or rise NDVI through time. According to figure 8, rapidly decreases take place at the transition areas between Binh Khanh - An Thoi Dong and An Thoi Dong - Ly Nhon. Other decreases are in Can Thanh. On the contrary, most of increase are observed in water areas. Some points of rapidly increases are in the core zone of mangrove forests.

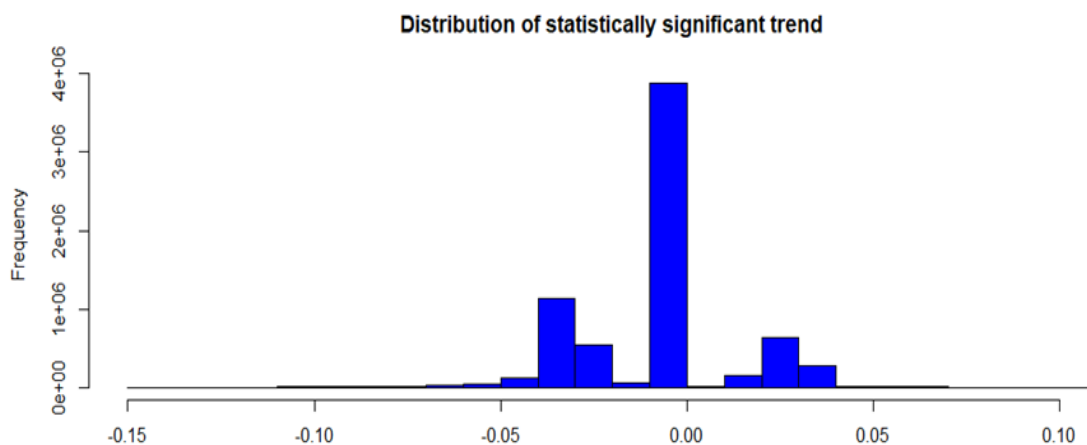


Figure 8a. Trending of NDVI change from 2015 to 2023.

Analyzing the spatial distribution results reveals specific points indicating a significant changes in NDVI, as determined by the linear regression model. The site exhibiting deposition tendencies from water flow demonstrates a statistically significant rise in NDVI. For instance, position 2 in Long Hoa and position 1 in Tam Thon Hiep showcase an increasing trend in NDVI. In other words, these sites have been continuously growth in mangrove forests over the past 9 years. Conversely, sites 3 and 4 experiencing NDVI declines denote consistent impacts over the same period, influencing the observed reduction in NDVI.

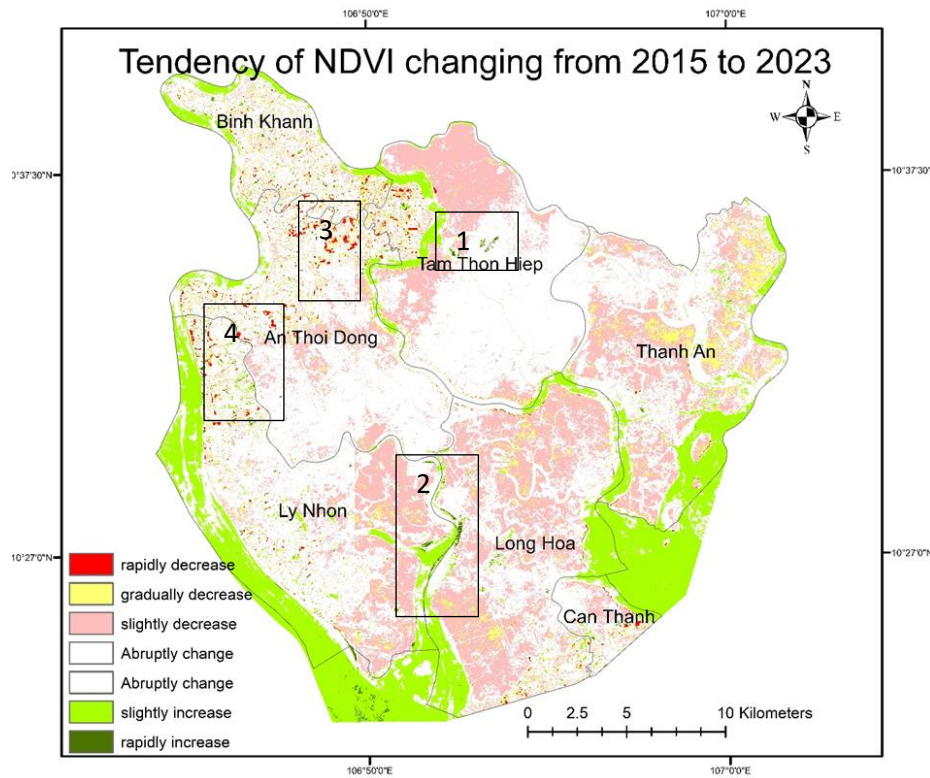


Figure 8b. Map of trending for NDVI change from 2015 to 2023.

3.4. Temporal analysis from 2015 to 2023

Table 2 indicates selected NDVI values which were extracted from random pixels, comparing to the associated p-values, slopes, and trends in NDVI changes. In brief, the trends observed are as follows: (1) NDVI exhibits either an increase or decrease without statistically reliable indications; (2) NDVI showcases either an increase or decrease with statistical reliability. However, in the linear regression analysis model, it demonstrates a consistent yearly increase or decrease in NDVIs. This suggests that pixels affected by sudden impacts resulting in abrupt NDVI changes will be omitted from the outcomes.

Table 2. Temporal analysis for NDVI from 2015 to 2023 at random sample point.

	Pixel	NDVI from 2015 to 2023									P-values	Slope values	Tendency
		2015	2016	2017	2018	2019	2020	2021	2022	2023			
1	1,000,000	0.55	0.24	0.39	0.32	0.22	0.2	0.35	0.23	0.1	0.03	-0.033	-0.03
2	1,500,000	0.14	0.12	0.25	0.44	0.36	0.43	0.43	0.49	0.29	0.04	0.034	0.03
3	1,755,000	-0.33	-0.23	-0.25	-0.19	-0.23	-0.21	-0.27	-0.16	-0.08	0.02	0.019	0.02
4	2,500,000	0.4	0.25	0.35	0.31	0.3	0.31	0.33	0.29	0.15	0.08	-0.015	0
5	2,755,000	0.49	0.58	0.66	0.63	0.69	0.62	0.68	0.48	0.38	0.43	-0.012	0
6	3,500,000	0.54	0.71	0.73	0.71	0.71	0.63	0.69	0.48	0.43	0.15	-0.022	0
7	3,555,000	0.26	0.58	0.68	0.58	0.64	0.55	0.63	0.43	0.38	0.95	-0.001	0
8	4,500,000	0.71	0.61	0.7	0.63	0.66	0.61	0.6	0.39	0.38	0.01	-0.037	-0.04
9	4,555,000	0.64	0.57	0.56	0.55	0.57	0.53	0.56	0.33	0.29	0.01	-0.035	-0.04
10	5,000,000	0.73	0.49	0.7	0.71	0.68	0.57	0.61	0.37	0.36	0.04	-0.037	-0.04

The graph in Figure 9 displays randomly selected NDVI values from specific pixels. Referring to the data table, these values are drawn from pixels positioned between the 1,500,000th and 4,500,000th. The graph represents the NDVI values across the years based on this selection. Utilizing linear regression analysis, three distinguished trends in the data emerge: gradually increase with a high R^2 correlation coefficient, low correlation with a low R^2 , and moderate correlation with an R^2 in the middle of range.

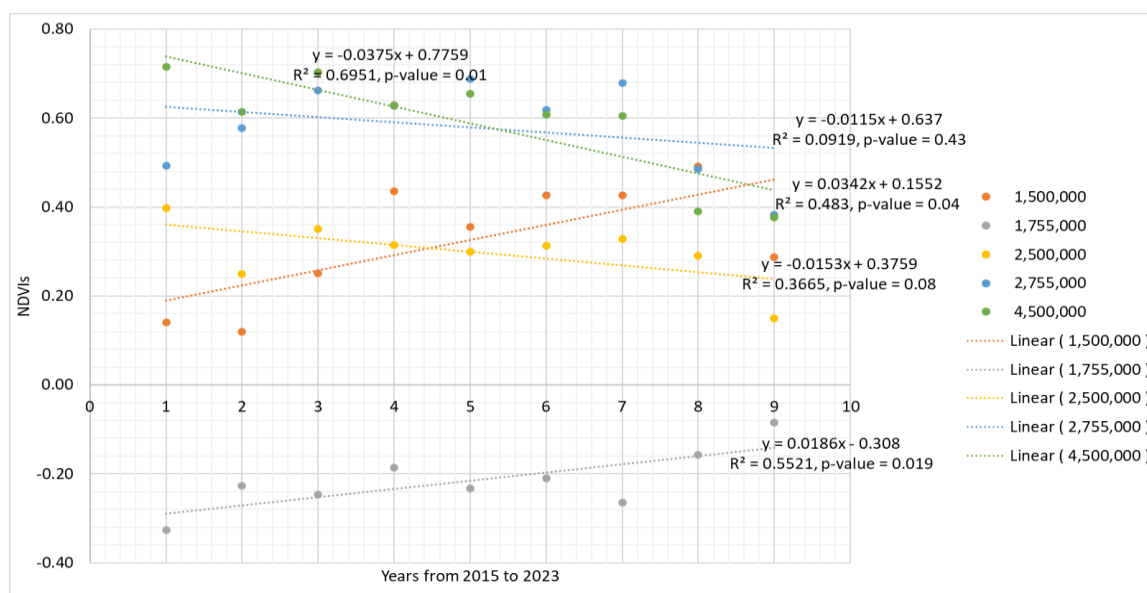


Figure 9. The linear regression for NDVI values at pixels.

Notably, the 4,500,000th pixel exhibits a significantly high R^2 value of 0.6951, while the 1,500,000th pixel shows a high increase over time with a medium R^2 of 0.483 and a p-value marginally reaching 0.04. At the 2,500,000th and 2,755,000th pixel, there's a consistent gradual reduction with a relatively R^2 of about 0.3665 and 0.0919, respectively. Similarly, p-values are insignificant in these two pixels. Thus, the more the R^2 value increases, the more the p-value tends to decrease below 0.05. However, the 1,755,000th pixel indicates that the R^2 slightly increase to 0.5521, while the p-value dramatically reduced to 0.019.

4. Conclusion

The results indicated that the decrease in average NDVIs from 2015 to 2023 was rationally deducible either from the downsizing of mangrove forest areas or the degradation of the mangrove forest. However, the annual NDVI statistic revealed there were areas with an acceleration of NDVI in comparison with the destruction of NDVI areas from 2015 to 2023. The significant declines occur rapidly at the transition zones between Binh Khanh and An Thoi Dong, as well as between An Thoi Dong and Ly Nhon. Additional declines are evident in Can Thanh. Conversely, the majority of increases are noted in aquatic regions. Certain locations exhibit rapid increases, particularly within the central core of mangrove forests.

This study presents a temporal statistical approach aimed at assessing NDVI changes within a defined timeframe. The main objective is not to quantify the direct expansion or reduction of mangrove forest areas. Instead, it seeks to indirectly evaluate mangrove forest quality through NDVI values in time series. Linear regression effectively models continuous processes like deposition or erosion. However, to evaluate other factors such as discrete human-made or sporadic impacts, alternative statistical models should be considered.

Notably, the unexpected increase in NDVI within water areas prompts further analysis, potentially associated with diverse processes like coastal erosion or deposition, environmental processes such as eutrophication and other influential factors that could impact these outcomes.

Author contribution statement: Conceived and designed the experiments; Analyzed and interpreted the data; contributed reagents, materials, analysis tools or data; manuscript editing: A.B.K.V.; Performed the experiments; contributed reagents, materials, analyzed and interpreted the data, wrote the draft manuscript: A.B.K.V.

Acknowledgements: The research utilized the available resources of Google Earth Engine (GEE), Sentinel-2 imagery, Geographic Information System (GIS), Google Earth, and the R programming packages, Ho Chi Minh City University of Natural Resources and Environment.

Competing interest statement: The authors declare no conflict of interest.

References

1. Shigeyuki, B. Studies in Can Gio mangrove biosphere reserve, Ho Chi Minh City, Viet nam. International Society for Mangrove Ecosystems (ISME), **2014**, *6*, ISSN 0919-2646.
2. Vinh, T.V.; Marchand, C.; Linh, T.V.K.; Jacotot, A.; Nho, N.T.; Allenbach, M. Soil and aboveground carbon stocks in a planted tropical mangrove forest (Can Gio, Vietnam). Chapter 12 in *Wetland Carbon and Environmental Management*, Wiley. **2021**, pp. 229–245. doi: 10.1002/9781119639305.ch12.
3. Torell, M.; Salamanca, A.M. Wetlands Management in Vietnam’s Mekong Delta: An Overview of the Pressures and Responses. *Environmental Science, Geography*, **2003**, pp. 1–19.
4. Vien, N.N.; Le, T.Q. Erosion and Accretion in Can Gio Mangroves. in *Studius in Can Gio Mangrove Biosphere Reserve, HCMC, Viet Nam. Int. Soc. Mangrove Ecosyst.* **2014**, *V6*, 31–36.
5. Hoan, H.D.; Kiet, B.N.T.; Binh, C.H.; Quy, P.V. Monitoring Riverbank Erosion in Can Gio mangroves. In *Studius in Can Gio Mangrove Biosphere Reserve, HCMC, Viet Nam*, **2014**, *V6*, 37–43.
6. Vien, N.N.; Le, S.V.; Miyagi, T.; Baba, S.; Chan, H.T. An Overview of Can Gio District and Mangrove Biosphere Reserve. **2014**. ISSN 0919-2646 *V6*.
7. Sugara, et al. Utilization of Sentinel-2 Imagery in Mapping the Distribution and Estimation of Mangroves’ Carbon Stocks in Bengkulu City. *Geosfera Indonesia* **2022**, *7(3)*, 219. Doi:10.19184/geosi.v7i3.30294.
8. Hirata, Y.; Tabuchi, R.; Patanaponpaiboon, P.; Pongparn, S.; Yoneda, R.; Fujioka, Y. Estimation of aboveground biomass in mangrove forests using high-resolution satellite data. *J. For. Res.* **2014**, *19(1)*, 34–41. Doi:10.1007/s10310-013-0402-5.
9. Vu, T.T.P.; Pham, T.D.; Saintilan, N.; Skidmore, A.; Luu, H.V.; Vu, Q.H.; Le, N.N.; Nguyen, H.Q.; Matsushita, B. Mapping Multi-Decadal Mangrove Extent in the Northern Coast of Vietnam Using Landsat Time-Series Data on Google Earth Engine Platform. *Remote Sens.* **2022**, *14*, 4664. <https://doi.org/10.3390/rs14184664>.
10. Meneses-Tovar, C. NDVI as indicator of degradation. *Unasyuva* **2011**, *62(2)*, 39–46.
11. Le, H.T.; Tran, T.V.; Gyeltshen, S.; Nguyen, C.P.T.; Tran, D.X.; Luu, T.H.; Duong, M.B. Characterizing Spatiotemporal Patterns of Mangrove Forests in Can Gio Biosphere Reserve Using Sentinel-2 Imagery. *Appl. Sci.* **2020**, *10*, 4058. <https://doi.org/10.3390/app10124058>.
12. Schmid, J.N. Using Google Earth Engine for Landsat NDVI time series analysis to indicate the present status of forest stands. Thesis for: Bachelor of Science, 2017, pp. 33. doi: 10.13140/RG.2.2.34134.14402/6.
13. Townsend, J.T. Theoretical analysis of an alphabetic confusion matrix*. *Percept Psychophys* **1971**, *9*, 40–50.
14. Kuhnert, M.; Voinox, A.; Spelt, R. Comparing raster map comparison algorithms for spatial modelling and analysis. *Photogramm Eng. Remote Sens.* **2005**, *71(8)*, 975–984.
15. Mchugh, M.L. Interrater reliability: the kappa statistic.
16. Ehsan, S.; Kazem, D. Analysis of land use-land covers changes using normalized

- difference vegetation index (NDVI) differencing and classification methods. *Afr. J. Agric. Res.* **2013**, *8*(37), 4614–4622. Doi:10.5897/ajar11.1825.
17. Nguyen, T.P.C.; Le, T.H.; Nguyen, T.O.; Le, C.L.; Ha, T.C. Vegetation Indices for Spatio-Temporal Analysis of the Quality of Can Gio Mangrove for Biodiversity and Conservation. Proceeding of the IOP Conference Series: Earth and Environmental Science, Institute of Physics. **2023**, *1247*(1), 012003. Doi: 10.1088/1755-1315/1247/1/012003.
 18. Lap, Q.K.; Luong, V.N.; Hong, X.T.; Tu, T.T.; Thanh, K.T.P. Evaluation of mangrove rehabilitation after being destroyed by chemical warfare using remote sensing technology: A case study in can gio mangrove forest in mekong delta, southern Vietnam. *Appl. Ecol. Environ. Res.* **2021**, *19*(5), 3897–3930. Doi: 10.15666/aeer/1905_38973930.
 19. Nguyen, H.H.; Quang, P.D.; Nguyen, V.D.; Linh, D.V.K.; Manh, N.K. Management of forest resources and environment estimation of mangrove carbon stocks using Sentinel 2a and field-based data in Tien Lang district, Hai Phong city. *Manage. Forest Resour. Environ.* **2020**, *10*, 48–58.
 20. Nguyen, S.T.; Bui, T.X.; Chau, D.T. Monitoring mangrove forest changes from multi-temporal Landsat Data in Can Gio Biosphere Reserve, Viet Nam. *Wetlands* **2016**, *212*, 635–640. Doi: 10.1007/s13157-016-0767-2.